

## Strong photoluminescence from Cr<sup>3+</sup> doped porous anodic alumina

This article has been downloaded from IOPscience. Please scroll down to see the full text article.

2004 J. Phys.: Condens. Matter 16 2463

(<http://iopscience.iop.org/0953-8984/16/13/024>)

View [the table of contents for this issue](#), or go to the [journal homepage](#) for more

Download details:

IP Address: 129.252.86.83

The article was downloaded on 27/05/2010 at 14:14

Please note that [terms and conditions apply](#).

# Strong photoluminescence from Cr<sup>3+</sup> doped porous anodic alumina

Tao Li, Shaoguang Yang<sup>1</sup>, Lisheng Huang, Jianrong Zhang, Benxi Gu and Youwei Du

National Laboratory of Solid State Microstructures, Nanjing University, Nanjing 210093, People's Republic of China

E-mail: sgyang@nju.edu.cn

Received 16 January 2004

Published 19 March 2004

Online at [stacks.iop.org/JPhysCM/16/2463](http://stacks.iop.org/JPhysCM/16/2463) (DOI: 10.1088/0953-8984/16/13/024)

## Abstract

Samples of Cr<sup>3+</sup> doped porous anodic alumina (PAA:Cr) with different crystal structures were prepared and very strong photoluminescence from a PAA:Cr template calcined at temperature higher than 900 °C was obtained. The crystallization of the PAA:Cr and its influence on the photoluminescence were studied. This kind of PAA:Cr with the template property and strong luminescence may be beneficial in the preparation of composite luminescent nanomaterial.

## 1. Introduction

In recent years, porous anodic alumina (PAA) with ordered nanopore arrays has attracted considerable attention due to its favourable applications as templates in fabricating nanocomposites [1–4]. Among the enriched properties of the nanostructured materials, including nanowires, nanotubes and nanodots, the light-emitting property is a fascinating topic with the development of the miniaturization of electronic and photonic devices. For instance, strong photoluminescence (PL) observed in ZnO nanowires was expected—an ultraviolet nanolaser [5]. Plenty of works have also been carried out on fabricating such nanosized photonic materials combined with the PAA template technique—ZnO, In<sub>2</sub>O<sub>3</sub>, TiO<sub>2</sub> and so on [6–9]. Also, nanomaterials with strong luminescence confined in PAA by a doping method have been reported—for example, Tb luminescence from titania xerogel [10].

Since the PAA template is one part of the nanocomposite, great attention should be paid to the light-emitting properties of PAA itself. Some studies have focused on this problem, and blue emission was obtained [4, 11]. In these works the PL observed in the PAA template was considered as the emission from the F (or F<sup>+</sup>) centres caused by the voids in PAA. This light-emitting property of the PAA template is beneficial in the development of the composite

<sup>1</sup> Address for correspondence: Department of Physics, Nanjing University, Nanjing, People's Republic of China.

photonic devices. As an insulator with a wide band gap, alumina itself provides a good matrix in which to implanting various ions, which has good prospects for achieving emitting properties.

In this paper, strong photoluminescence was observed in PAA:Cr prepared by doping  $\text{Cr}^{3+}$  in PAA with a calcination temperature higher than  $900^\circ\text{C}$ . The PL peaks locate at about 694 nm, corresponding to the R-line of ruby, which indicates the doping of  $\text{Cr}^{3+}$  in  $\text{Al}_2\text{O}_3$ . The crystallization process of PAA:Cr $^{3+}$  and the relationship between the PL intensity and its crystal structure were investigated. Although the light-emitting properties have been widely and intensively studied in other forms of  $\text{Al}_2\text{O}_3$  with ion implantation [12–18], such fascinating PL in the PAA template has rarely been reported. This work presents a novel method for improving the light-emitting properties of PAA template, which may be helpful in the development of luminescent devices.

## 2. Experimental details

Firstly, aluminium foil (99.999%) was annealed at  $500^\circ\text{C}$  for 5 h in Ar atmosphere, and then degreased by immersion in ethanol for about 10 min, etched in 5 wt% NaOH at room temperature for 5 min to remove the native oxide and washed thoroughly with distilled water. Afterwards, the aluminium foil was anodized at  $50\text{ V}_{\text{dc}}$  for 6 h in  $0.3\text{ mol l}^{-1}$  oxalic acid. After anodizing, the product was exposed to a  $\text{CuCl}_2$  solution to remove the remaining aluminium; this was followed with a pore widening process achieved by immersion in 6 wt% phosphoric acid solution for 30 min. The nearly transparent PAA sheet obtained was put into 20 wt%  $\text{Cr}_2(\text{SO}_4)_3$  solution for about 30 min. After the liquor at the surface had been wiped off carefully using filter paper, the PAA with  $\text{Cr}_2(\text{SO}_4)_3$  inside the nanopores was dried in air. Then, a series of samples were prepared by calcining at 700, 800, 900, 950, 1000 and  $1250^\circ\text{C}$  for 10 h. After the calcination, the samples calcined at 700 and  $800^\circ\text{C}$  kept the original transparent appearance with a weak green colour due to the small amount of remaining  $\text{Cr}_2\text{O}_3$ , while the others turned pink, which indicated the doping with the  $\text{Cr}^{3+}$ .

A scanning electron microscope (SEM JSM5610LV) was used in characterizing the morphology of the PAA:Cr. A UV–vis–NIR spectrometer (Hitachi U-3400) was employed in the light absorption measurement in the range of ultraviolet–visible frequencies. Photoluminescence spectra measurements were performed in a confocal laser micro-Raman spectrometer (Raman, LABRAM-HR) with 488 nm laser excitation. X-ray diffraction (XRD Rigaku D/Max-RA) analysis with Cu  $K\alpha$  radiation and differential thermal analysis (DTA) were carried out to investigate the structures and crystallization process of the  $\text{Cr}^{3+}$  doped PAAs.

## 3. Results and discussion

Figure 1 shows the strong and narrow room temperature photoluminescence of the sample calcined at  $1000^\circ\text{C}$ . The left inset is an enlargement near 694 nm wavelength with the doublet R-lines of ruby located at 693 and 694.5 nm, which reveals the  ${}^2\text{E}-{}^4\text{A}_2$  transitions. The PL spectrum indicates the possibility of  $\text{Cr}^{3+}$  ions being doped into the PAA template as it is crystallized to the  $\alpha\text{-Al}_2\text{O}_3$  phase. The weak, long wavelength wing of the inhomogeneously broadened R-line can be connected with the vibronic transitions [13]. The subsequent UV–visible absorption spectrum also confirms the doping of the  $\text{Cr}^{3+}$  in the octahedral site of  $\alpha\text{-Al}_2\text{O}_3$ , as shown in figure 2. Three strong absorption bands with peak positions at 235, 410 and 563 nm are observed, corresponding to the three electron transitions of  $\text{Cr}^{3+}$  in  $\alpha\text{-Al}_2\text{O}_3$ :  ${}^4\text{A}_2-{}^4\text{T}_1(\text{P})$ ,  ${}^4\text{A}_2-{}^4\text{T}_1(\text{F})$  and  ${}^4\text{A}_2-{}^4\text{T}_2$ , respectively [19]. The weak absorption at 695 nm is for the well-known transition of  ${}^4\text{A}_2-{}^2\text{E}$ , which is coincident with the narrow peaks in the PL

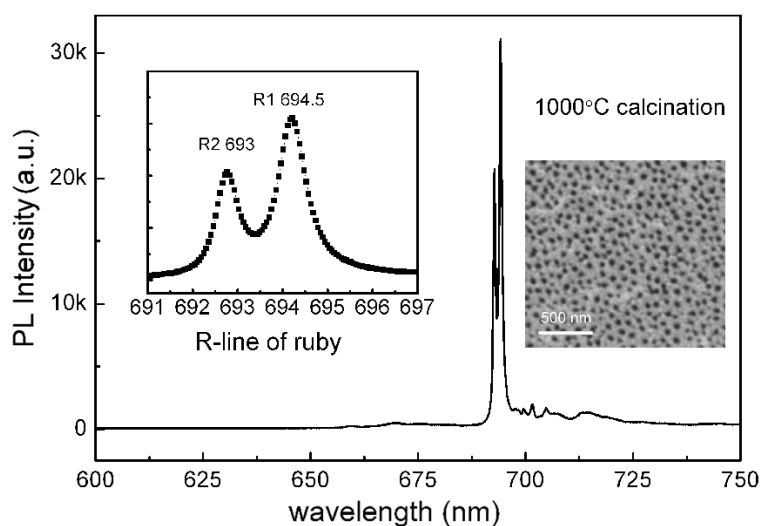


**Figure 1.** The PL spectrum of the Cr<sup>3+</sup> doped PAA template calcined at 1000 °C. The left inset is an enlargement near 694 nm wavelength. The right inset shows the SEM image of the template, top view, with a pore diameter of about 60 nm.

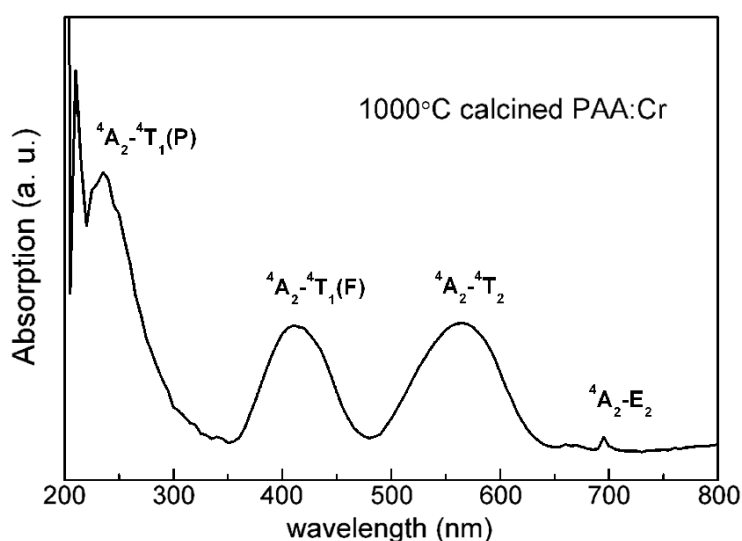


**Figure 2.** The UV-visible absorption spectrum of the PAA:Cr calcined at 1000 °C.

spectrum. The right inset of figure 1 shows the SEM image of the PAA:Cr template calcined at 1000 °C, top view. From the figure, it is seen that there is good nanopore array with pore diameter of about 60 nm, which indicates the feasibility of template application. It should be pointed out that when the calcination temperature reached 1250 °C, the PAA template collapsed on the surface, as observed by the SEM.

For further investigation, Cr<sup>3+</sup> doped PAA samples with different crystalline phases were prepared at various calcination temperatures for 10 h. XRD patterns of a series samples are shown in figure 3. It can be clearly seen that the PAA calcined at 700 °C remains amorphous.

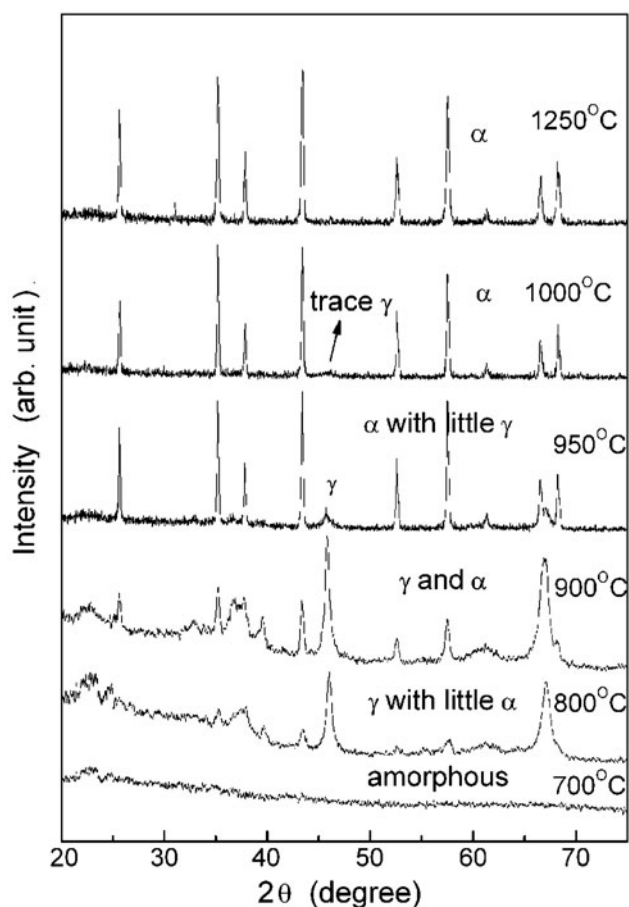
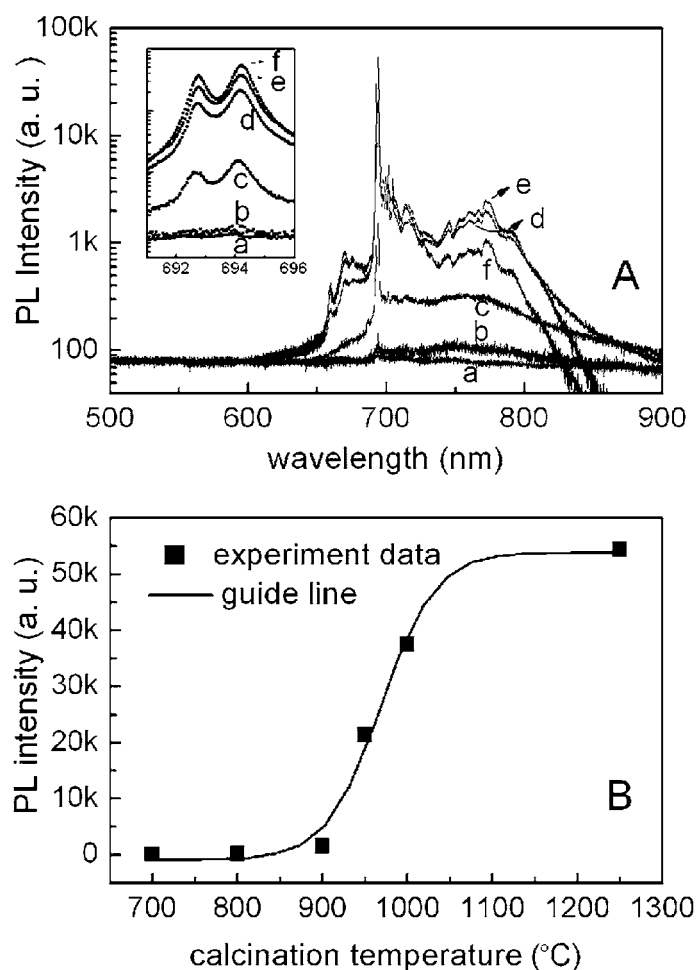


Figure 3. XRD patterns of the PAA:Cr samples with different calcination temperatures.

When the calcination temperature increases from 800 to 1250 °C, the PAA crystallizes and the structure experiences a transition from the  $\gamma$  to the  $\alpha$  phase. There is coexistence of  $\alpha$  and  $\gamma$  phases in the samples calcined at 800, 900 and 950 °C, but the PAA:Cr sample calcined at 1000 °C reveals a very pure  $\alpha$ -Al<sub>2</sub>O<sub>3</sub> phase, though a trace  $\gamma$  phase remains. This temperature of transition from the  $\gamma$  to the  $\alpha$  phase is much lower than that in previous reports [20], which may be related to the particular PAA property caused in the anodizing process. Figure 4(A) shows PL spectra of the PAA:Cr samples calcined at different temperatures and figure 4(B) shows luminescence intensities as a function of the calcination temperature. From the figures, it is found that photoluminescence spectra of the samples with corresponding structures show remarkable changes in PL intensities. Since the strongest intensity of the R-line is more than 10 000 times larger than the weakest one, the logarithm is used on the intensity axis to make the spectra more clearly distinguished. The drastic increase in PL intensity of  ${}^2E-{}^4A_2$  transitions in the samples for calcination temperature from 900 to 1250 °C corresponds to the production of the Cr<sup>3+</sup> doped  $\alpha$ -Al<sub>2</sub>O<sub>3</sub>. Another noticeable detail is that the intensity of the long wavelength band for the sample calcined at 1250 °C decreases compared with the ones at 1000 and 950 °C. According to the previous research, the broad band may come from the vibronic transitions in disordered crystal, such as  $\gamma$  or  $\delta$  phases in Al<sub>2</sub>O<sub>3</sub> [13]. In present work, the remaining  $\gamma$ -Al<sub>2</sub>O<sub>3</sub>



**Figure 4.** (A) PL spectra of the PAA:Cr samples calcined at (a) 700 °C, (b) 800 °C, (c) 900 °C, (d) 950 °C, (e) 1000 °C and (f) 1250 °C. The inset is an enlargement of the R-line. (B) Luminescence intensities as a function of the calcination temperature.

should be the main cause of the broad long wavelength band. When the calcination temperature increases to 1250 °C, the further phase transition of Al<sub>2</sub>O<sub>3</sub> from  $\gamma$  to  $\alpha$  leads to a further reducing of the trace  $\gamma$  phase content, resulting in the decrease of the broadband intensity.

Differential thermal analysis (DTA) of Cr<sup>3+</sup> doped PAA is performed and the result is shown in figure 5. A sharp peak is observed at 900 °C, which indicates a strong phase transition. Taking this in combination with the XRD patterns of the samples, it can be concluded that this peak relates to the  $\gamma$  to  $\alpha$  phase transition. Since the XRD peaks of the  $\gamma$  phase are already very strong for the sample calcined at 800 °C, the crystallization process should start from below 800 °C and the sharp peak at 900 °C in the DTA curve cannot be the crystalline peak of the  $\gamma$  phase. The remaining  $\gamma$  phase in the samples calcined at 900 and 950 °C may be explained as a result of retardation of the phase transition. From figure 4(B), we can readily see the drastic increase of the PL intensity at around 950–1000 °C, which can contribute to the completion of the transition of  $\gamma$ -Al<sub>2</sub>O<sub>3</sub> to  $\alpha$ -Al<sub>2</sub>O<sub>3</sub>. Such a process is also in agreement with the DTA result.

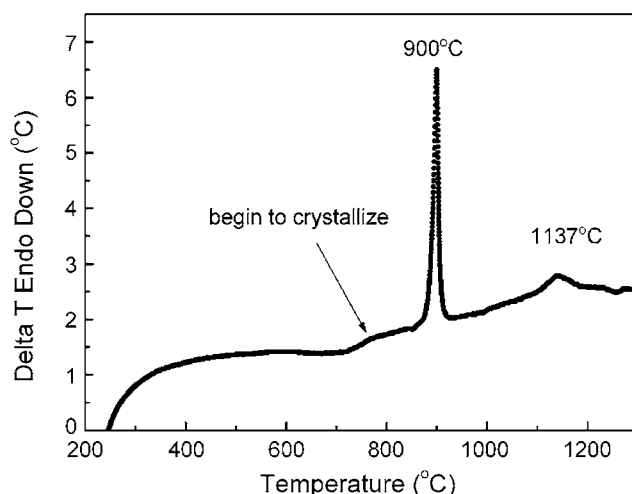


**Figure 5.** The differential thermal analysis (DTA) curve for the PAA:Cr.

Furthermore, for the increase of R-line intensity, the increase of doped  $\text{Cr}^{3+}$  with rising calcination temperature should be taken into account. Because the intensities of the broad long wavelength band enhance monotonically with the temperature from 900 to 1000 °C, the amount of doped  $\text{Cr}^{3+}$  should increase, considering the reduction of the amount of  $\gamma$  phase  $\text{Al}_2\text{O}_3$ . However, the completion of the  $\gamma$  to  $\alpha$  transition is still the dominant cause of the strong red photoluminescence.

Although we find that the sample calcined at 1250 °C has the best light-emitting properties, from figure 4, the pore array structure is partly destroyed as mentioned above and it is much more fragile than the 1000 °C one. In other words, the trace  $\gamma$  phase in PAA:Cr is helpful in preserving the template properties. Thus template application of the PAA:Cr calcined at 1000 °C is feasible due to its good pore array morphology. The fascinating optical property of PAA:Cr obtained indicates the possibility of controlling the light emission by doping with various ions. Such a method could also be employed in fabricating excellent nanomaterials by depositing versatile materials into the template. Moreover, the  $\text{Cr}^{3+}$  doped PAA template shows a much lower  $\alpha$  transition temperature, which may be convenient for fabrication and production.

#### 4. Conclusion

In summary, PL spectra from  $\text{Cr}^{3+}$  doped PAA templates calcined at different temperature were investigated and the strong R-line of ruby was observed for high temperature calcined samples. XRD and DTA results reveal the crystallization and phase transition process of the PAA:Cr, which affects its light-emitting properties greatly. SEM observation showed that the sample calcined at 1000 °C has good nanopore structure, ensuring its applicability as a template. The strong photoluminescence and low  $\gamma$  to  $\alpha$  transition temperature of the PAA:Cr reveals great potential for applications in nanocompositions of photonic devices and optical materials.

#### Acknowledgments

This work was supported by the Natural Science Foundation of Jiangsu Province under Grant No BK2001404 and the National Key Project of Fundamental Research of China No G1999064508.

## References

- [1] Masuda H and Fukuda K 1995 *Science* **268** 1466
- [2] Masuda H, Yamada H, Satoh M and Asoh H 1997 *Appl. Phys. Lett.* **71** 2770
- [3] Jessensky O, Müller F and Gösele U 1998 *Appl. Phys. Lett.* **72** 1173
- [4] Du Y, Cai W L, Mo C M, Chen J, Zhang L D and Zhu X G 1999 *Appl. Phys. Lett.* **74** 2951
- [5] Huang M H, Mao S, Feick H, Yan H Q, Wu Y Y, Kind H, Weber E, Russo R and Yang P D 2001 *Science* **292** 1897
- [6] Li Y, Meng G W, Zhang L D and Phillipp F 2000 *Appl. Phys. Lett.* **76** 2011
- [7] Wang Z and Li H L 2002 *Appl. Phys. A* **74** 201–3
- [8] Zheng M J, Zhang L D, Li G H, Zhang X Y and Wang X F 2001 *Appl. Phys. Lett.* **79** 839
- [9] Lei Y, Zhang L D, Meng G W, Li G H, Zhang X Y, Liang C H, Chen W and Wang S X 2001 *Appl. Phys. Lett.* **78** 1125
- [10] Gaponenko N V, Davidson J A, Hamilton B, Skeldon P, Thompson G E, Zhou X and Pivin J C 2000 *Appl. Phys. Lett.* **76** 1006
- [11] Huang G S, Wu X L, Mei Y F, Shao X F and Siu G G 2003 *J. Appl. Phys.* **93** 582
- [12] Wen Q, Clarke D R, Yu N and Nastasi M 1995 *Appl. Phys. Lett.* **66** 293
- [13] Kulinkin A B, Feofilov S P and Zakharchenya R I 2000 *Phys. Solid State* **42** 857
- [14] Tkhek-de I, Lyamkina N E, Lyamkin A I, Podavalova O P, Slabko V V and Chiganova G A 2001 *Tech. Phys. Lett.* **27** 533
- [15] Yu Z Q, Li C and Zhang N 2002 *J. Lumin.* **99** 29
- [16] Monteiro T, Boemare C, Soares M J, Alves E, Marques C, McHargue C, Ononye L C and Allard L F 2002 *Nucl. Instrum. Methods B* **191** 638
- [17] Krishnan R, Kesavamoorthy R, Dash S, Tyagi A K and Raj B 2003 *Scr. Mater.* **48** 1099
- [18] Yu H J and Clarke R 2002 *J. Am. Ceram. Soc.* **85** 1966
- [19] Lumb M D 1978 *Luminescence Spectroscopy* (New York: Academic)
- [20] Feofilov S P, Kaplyanskii A A and Zakharchenya R I 1995 *J. Lumin.* **66/67** 349